Defense Technical Information Center Compilation Part Notice

ADP014037

TITLE: Fiber Optic Distribution Networks for Military Applications

DISTRIBUTION: Approved for public release, distribution unlimited
Availability: Hard copy only.

This paper is part of the following report:

TITLE: Optics Microwave Interactions [Interactions entre optique et micro-ondes]

To order the complete compilation report, use: ADA415644

The following component part numbers comprise the compilation report:
ADP014029 thru ADP014039

Fiber Optic Distribution Networks for Military Applications

Afshin S. Daryoush
Department of Electrical and Computer Engineering
Drexel University, Philadelphia, PA 19104, USA

Daryoush@ece.drexel.edu

ABSTRACT

A number of military applications require ad-hoc wireless communication and networking systems that employ low phase noise reference signals for up- and down-conversion of communication signals and further processing of data signals. High performance fiber optic link s are important for distribution of signals while phase noise degradation induced by AM-PM conversion in fiberoptic links impacts phase coherency of local oscillator (LO) signals in distributed systems. This paper focuses on issues associated with directly and externally modulated fiber optic links and their performance limitations in terms of gain, noise figure, nonlinearity, and dynamic range. The performance-cost aspects of both types of links are compared and it is pointed out that directly modulated links meet performance-cost requirements in most applications. Analysis of phase noise degradation of frequency reference is presented for directly modulated fiber optic distribution networks. SRS induced fiber nonlinearity is also discussed. Since the response of a Fabry-Perot laser diode can be altered by adding an external feedback, resulting in a resonance peak, results of a monolithically integrated FP laser are discussed. Finally, opto-electronic mixing of IF and LO signals are also demonstrated for the mode-locked case.

1.0. INTRODUCTION

Recently a lot of efforts has been directed toward increase in global interconnectivity through electronic media and many market studies has identified a significant increase in demand for personal communication services in the 21st century. One of the most important proponents of this market is in the inter-office communication, where the high-speed fiberoptic local area networks (LAN) are combined with wireless communication to provide interconnectivity among many users.

Conceptual system architecture of a hybrid wireless and fiber optic LAN with applications to both civilian and military systems is shown in Fig. 1. In this figure, personal computers (PC) are networked together through this hybrid wireless and fiberoptic networks. The digital data from the PC is up-converted by a millimeter wave (MMW) stable carrier and is then radiated by a low cost omni-directional antenna. The modulated received RF signal is then down-converted to the coded digital signals using the same stabilized MMW local oscillator (LO). The coded digital signal is then networked to other users through a high-speed fiberoptic network. The fiber-optic LAN is envisioned to operate either in analog format or digital data rates well above Gb/s.

An important component of a reliable inter-office communication for the portable PC is the use of the low power consuming frequency translation circuits, which up- and down-converts the information without any degradation in the its spectral purity. Frequency stability of the local oscillators used in the MMW wireless communication, and the clock recovery circuits used in the decision circuits, are critical in accurate data retrieval.

Paper presented at the RTO SET Lecture Series on "Optics Microwave Interactions", held in Jouy en Josas, France, 2-3 September 2002; Duisburg, Germany, 5-6 September 2002; Budapest, Hungary, 9-10 September 2002, and published in RTO-EN-028.

This paper first reviews the performance of directly and externally modulated fiber optic links. First analytical expressions are presented for gain, noise figure, and dynamic range and sources of phase noise degradation in directly and externally modulated FO links are presented. Cost and reliability performance of fiberoptic links in harsh military environment is also reviewed. Next performance of a long F-P laser structure that is monolithically integrated with electro-absorption modulator is reviewed where efficient transmission of data and carrier signals with high SFDR and low phase noise degradation are achieved.

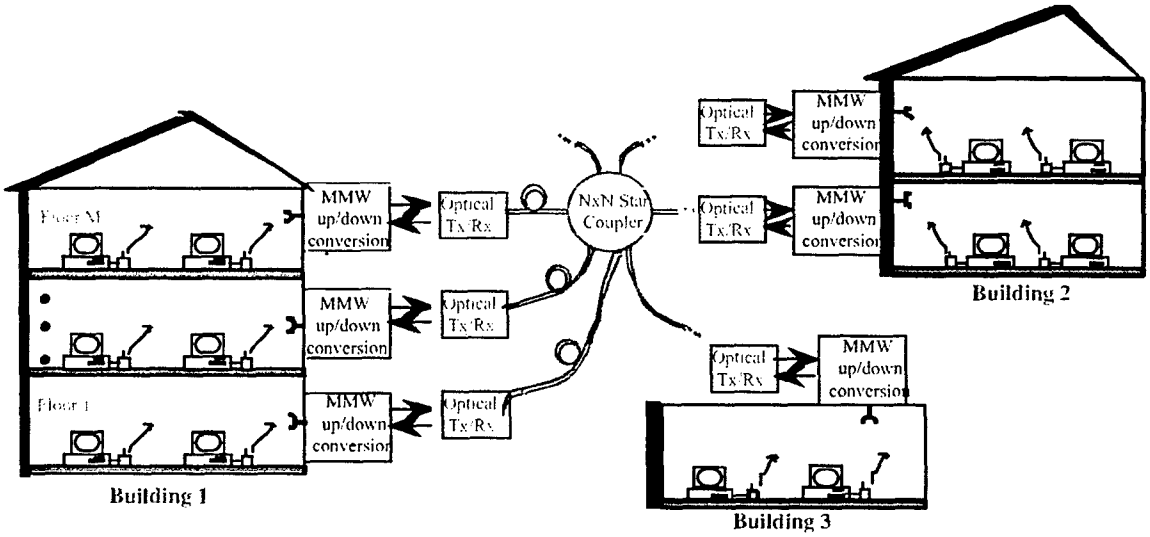

Fig. 1. Conceptual diagram of hybrid fiberoptic and wireless local area distributed network system. (═══ Optical fiber distribution, ——— electrical distribution, ⇝ free space distribution).

2.0. FO LINK PERFORMANCE

Fiber optic (FO) links are employed for distribution of frequency reference as well data communications in distributed systems, where these links need to provide RF signals with high dynamic range and low phase noise degradation. The FO link gain and noise performance will impact signal to noise performance, while the nonlinearity of various elements in the optical system will contribute to a limited dynamic range. The nonlinear phase and amplitude variation with input RF power will results in AM-AM and AM-PM conversion.

Directly Modulated FO Link: The gain of a fiber-optic link can be calculated in terms of microwave scattering parameters using the signal flow diagram (SFD) technique [1]. The transducer gains of the optical transmitter and optical receiver are derived separately and then combined to yield the gain of the complete link. The link gain is expressed as

$$G = \frac{P_{out,Tx}}{P_{av,\,Rx}} = G_{Tx} \times |H_L|^2 \times G_{Rx}$$

$$= \frac{|S_{21D}|^2 \; |S_{21L}|^2 \, (1 - |\Gamma_{las}|^2) \; (\eta_L K_L L K_D \eta_D)^2}{|1 - \Gamma_{las} \, S_{22L}|^2 \; |1 - \Gamma_{SD} \, S_{11D}|^2} \, .$$

When a directly modulated semiconductor laser diode is employed in the optical transmitter, the SFD is obtained by considering the forward-bias junction resistance of the laser diode to be the port two termination of a two-port network consisting of the microwave impedance-matching and driving circuit combined with the other device

parameters of the laser. Whereas a reverse-biased p-i-n photodiode is employed in the optical receiver, the SFD is obtained by considering the junction resistance of the diode to be the port one terminating load to a two-port network consisting of the microwave impedance-matching circuit and the other device parameters of the detector. The link current transfer function, H_L, is defined as the ratio of detector current to RF current across the laser. This is a measurable quantity that is a function of the electro-optic device quantum efficiencies as well as optical attenuation and coupling efficiency, where η_L is the laser diode external quantum efficiency, η_D is the detector responsivity, L is the optical attenuation in the fiber, and K_L, K_D are the laser-to-fiber and fiber-to-detector coupling efficiencies, respectively. At the moment nonlinear fiber performance due to Stimulated Brillouin and Raman Scattering processes for long fiber length L is ignored, but this issue is to be discussed later.

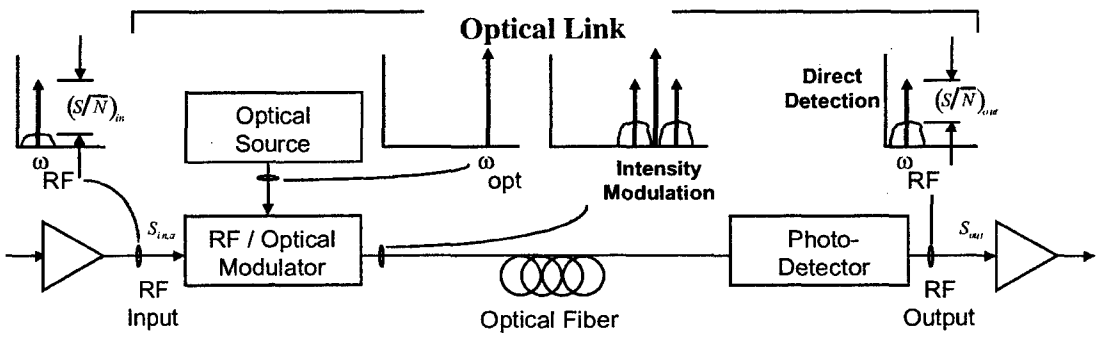

Fig. 2. Overall structure of a fiberoptic link. Note for directly modulated system the optical source is internally modulated whereas in externally modulated link the electro-optic property is used to perform intensity modulation in a MZ modulator.

The four contributions to the noise power of the directly modulated fiber-optic link. The total noise power at the output of the detector is the sum of all these individual noise powers,

$$N_{out} = N_{RIN} + N_{shot} + N_{thtx} + N_{thrx} = N_{RIN} + N_{shot} + N_{th}.$$

The dominant term is the laser RIN noise power, which is expressed as:

$$N_{RIN} = RIN(f)\,(I_b - I_{th})^2\,(\eta_L K_L L K_D \eta_D)^2 \frac{|S_{21D}|^2}{|(1 - \Gamma_{SD} S_{11D})|^2} B Z_0$$

The next dominant noise source is shot noise of the detector, including dark current noise,

$$N_{shot} = 2e\left[(I_b - I_{th})(\eta_L K_L L K_D \eta_D) + I_d\right] B \frac{|S_{21D}|^2}{|(1 - \Gamma_{SD} S_{11D})|^2} Z_0$$

followed with the thermal noise of the transmitter,

$$N_{thtx} = 4kT_a B\,(\eta_L K_L L K_D \eta_D)^2\, Re\{Y_{thl}\} \frac{|S_{21D}|^2}{|(1 - \Gamma_{SD} S_{11D})|^2} Z_0$$

Finally the thermal noise of the detector,

$$N_{thrx} = 2kT_a B\left(1 - |\Gamma_{in}|^2\right).$$

The only noise source at the input of the link is the thermal noise in the transmitter circuitry; i.e., $N_{in} = kT_aB$. Noise Figure of the fiber-optic link is defined as

$$NF_{Link} = \frac{(SNR)_i}{(SNR)_o} = \frac{P_{in} * N_{out}}{P_{out} * N_{in}} = \frac{1}{G_{Link}} * \frac{N_{out}}{N_{in}} \qquad (1)$$

Externally Modulated FO Link: The small-signal gain of an externally modulated fiber-optic link is derived using the SFD technique as was applied to direct modulation. When a Mach-Zehnder interferometric modulator is employed in the optical transmitter to impress a microwave signal upon the optical carrier in a single-mode fiber, the transmitter SFD is obtained by considering the capacitance C_M across the modulator terminals to be the port two termination of a two-port network consisting of the microwave impedance-matching circuit and the other device parameters in the equivalent circuit of the modulator. The output power of a fiber-optic link depends on the amplitude of photocurrent, I_{det}, generated in the detector, which is in turn proportional to the RF voltage V_M across the capacitor C_M. This gain is represented as:

$$G = \left(\frac{\pi L K_D \eta_D P_{in,op} Z_0}{2 V_\pi}\right)^2 \frac{|S_{21M}|^2 |S_{21D}|^2 |1+\Gamma_M|^2}{|1 - S_{22m}\Gamma_M|^2 |1 - S_{11D}\Gamma_{SD}|^2}.$$

Where V_π = bias voltage required for 100% modulation and $P_{in,op}$ is the optical output of the modulator. Figure 3 compares the achievable gain of directly and externally modulated fiber optic links. Note that a higher gain is achieved when optical source and detector with efficient light coupling and responsivity are employed. Finally, gain of the externally modulated FO link monotonically increases as optical power squared. Four noise sources contribute to the output noise power of the link. The dominant term in the case of large input optical power is the shot noise followed with excess RIN noise of the laser. The shot noise of the detector, including dark current, is expressed as:

$$N_{shot} = 2e\left[\left(\frac{\eta_{op}\eta_D P_{in,op}}{2}\right) + I_d\right] B \frac{|S_{21D}|^2}{|1 - \Gamma_{SD} S_{11D}|^2} Z_0$$

The excess noise of the laser is related to optical source RIN noise which could be significantly lower than the semiconductor laser diode.

$$N_{excess} = \left[RIN\left(\frac{\eta_{op}\eta_D P_{in,op}}{2}\right) - 2e\right] \times \left(\frac{\eta_{op}\eta_D P_{in,op}}{2}\right) B \frac{|S_{21D}|^2}{|1 - \Gamma_{SD} S_{11D}|^2} Z_0$$

The thermal noise sources of the transmitter and of the detector are presented respectively as:

$$N_{thtx} = kT_a B \left(\frac{\pi \eta_{op}\eta_D P_{in,op} Z_0}{2 V_\pi}\right)^2 \frac{|S_{21m}|^2 |S_{21D}|^2 |1+\Gamma_M|^2}{|1 - \Gamma_M S_{22m}|^2 |1 - \Gamma_{SD} S_{11D}|^2}$$

$$N_{thrx} = 2kT_a B \left(1 - |\Gamma_{in}|^2\right)$$

The total noise power at the output of the detector is the sum of all these individual noise powers. As in the direct modulation case, the noise power at the input to the external modulation link is simply $kT_a B$. Therefore the noise figure is given by equation (1). Note the total shot noise increases as optical power, therefore signal to noise ration increases as optical power increases in the externally modulated links. However, the challenge is developing high-speed high-power handling photodetectors.

Fig. 3 depicts comparison measured and analytical calculated gain results of directly and externally modulated fiberoptic links. The optical power can be high in externally modulated fiberoptic links when a solid state laser is employed as optical source. Note a low V_π MZ modulator and operation in the quadrature point of $V_b = V_\pi/2$ (i.e., $\phi=90°$) along with a high power handling photodiode allows for the highest reported gain for FO links. Naturally a higher responsivity (i.e. η_L and η_D) laser diode and photodiode result in a lower insertion loss.

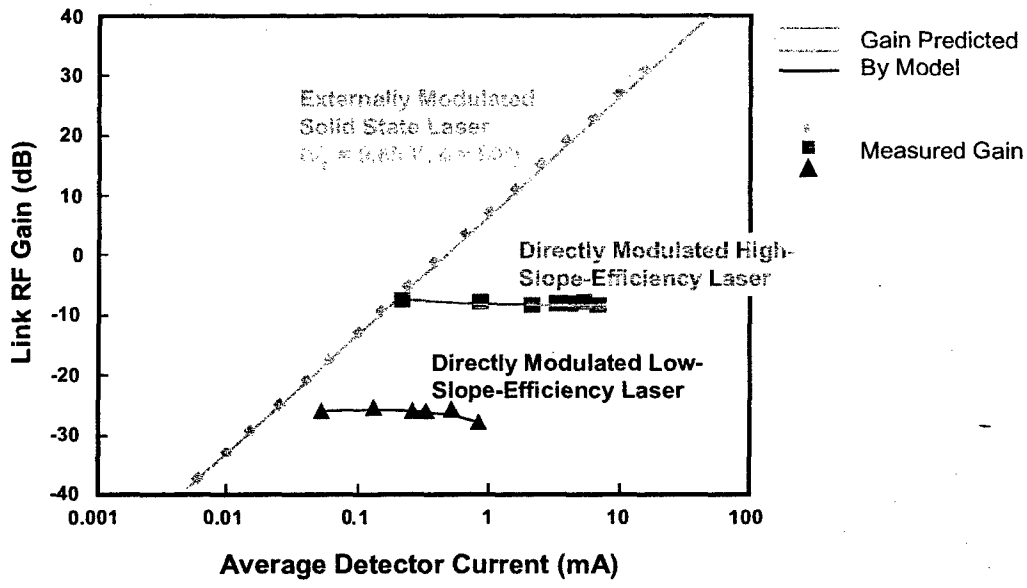

Fig. 3. Comparison of experimental and simulation results of directly and externally modulated fiber optic links at HF [2]. (Courtesy of Ed Ackerman of Photonics Inc).

Dynamic Range: Spurious free and compression dynamic range are directly related to linearity off the optical modulator (i.e., laser diode in the case of directly, and MZ modulator in the externally modulated FO links). The 3rd order intercept point and 1 dB compression point for the directly modulated are calculated [1] based on the optical modulation index m,

$$P_{in,int} = \frac{m_{int}^2 (I_b - I_{th})^2 \left| 1 - S_{22L}\Gamma_{Las} \right|^2 Z_0}{\left| S_{21L} \right|^2 \left(1 - \left| \Gamma_{Las} \right|^2\right)}$$

$$P_{in,1dB\ CP} = \frac{m_{1dB\ CP}^2 (I_b - I_{th})^2 \left| 1 - S_{22L}\Gamma_{Las} \right|^2 Z_0}{\left| S_{21L} \right|^2 \left(1 - \left| \Gamma_{Las} \right|^2\right)}$$

In a similar fashion, the 3rd order intercept point and 1 dB compression point are derived for externally modulated fiberoptic links as:

$$P_{in,int} = \frac{8\, V_\pi^2 \left| 1 - S_{22m}\Gamma_M \right|^2}{\pi^2 Z_0 \left| S_{21m} \right|^2 \left| 1 + \Gamma_M \right|^2}$$

$$P_{in,1dB\ CP} = \frac{0.950454^2\, V_\pi^2 \left| 1 - S_{22m}\Gamma_M \right|^2}{\pi^2 Z_0 \left| S_{21m} \right|^2 \left| 1 + \Gamma_M \right|^2}$$

Using the derived relationship for intercept and compression points, Spurious Free and compression dynamic range are calculated using the following expressions:

$$SFDR = \frac{2}{3} \times 10\, Log_{10}\left[\frac{P_{out,int}}{kT_aG\ NF}\right]\ dB.Hz^{2/3}$$

$$CFDR = 10\, Log_{10}\left[\frac{P_{out,1dB\ CP}}{kT_aG\ NF}\right]\ dB.Hz$$

Fig. 4 represents the calculated dynamic range of externally and directly modulated fiberoptic links as a function of frequency and makes comparison against the measured results at various operating frequencies. Moreover, references are made to various practical military and civilian applications at those frequency bands. As seen the externally modulated fiber optic link with high power and low RIN noise solid state laser as source combined with high power handling photodetectors provide for the highest dynamic range. However, note that at lower frequencies, externally modulated link using DFB lasers as source outperforms solid state laser due to its RIN resonance peak about MHz. In the directly modulated links, a higher dynamic range is obtained in DFB laser based systems where a lower RIN noise is obtained compared to FP laser diodes.

On the other hand, Fig. 5 compares cost vs DR performance of directly and externally modulated links reported. The dashed line corresponds to the current cost-performance limit of the reported FO links. In addition a number of civilian applications are identified in this figure. As indicated, even though externally mdulated links will meet the stringent requirements of many commercial applications, however due to its high-cost can not be considered economically viable. Therefore, the derive needs to be either improving performance of directly modulated links or through manufacturing innovations drive the price of externally modulated links down.

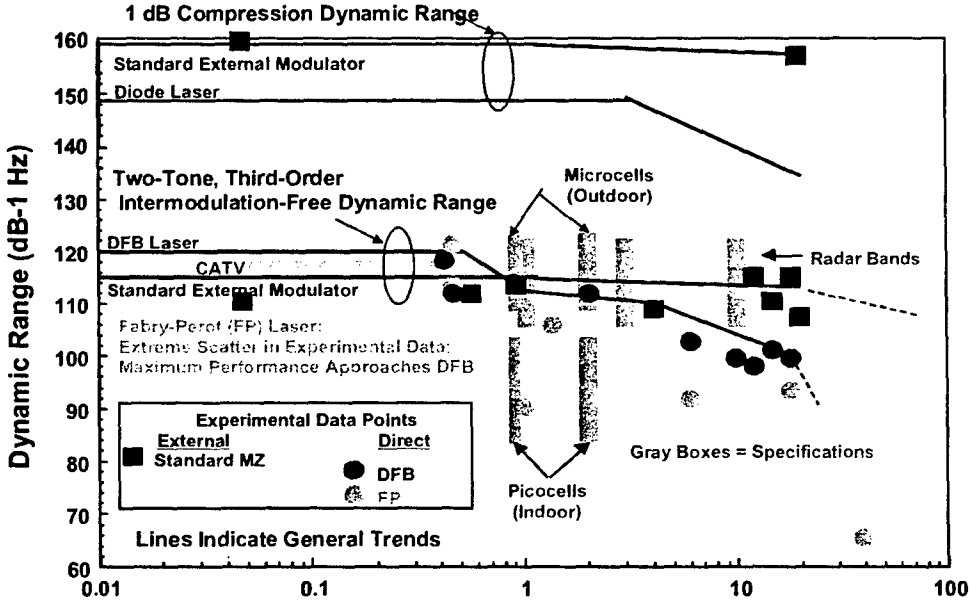

Fig. 4. Comparison of measured and calculated dynamic range for directly and externally modulated fiber optic links [2]. (Coustesy of Ed. Ackerman of Photonics Inc.)

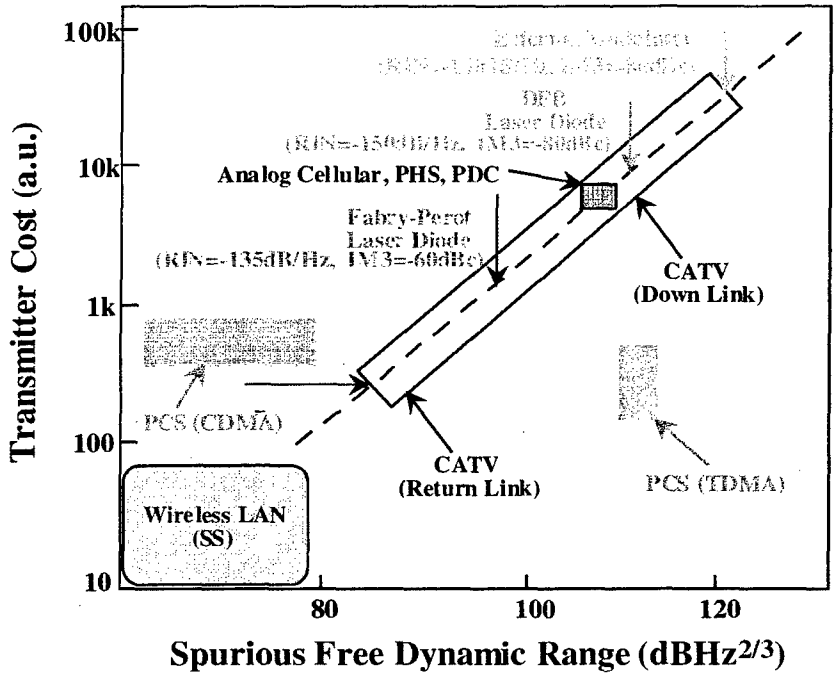

Fig. 5. Cost-Dynamic Range comparison of directly and externally modulated fiber optic links for a variety of civilian applications [3].

Fiber Nonlinearity: WDM optical systems are employed in optically controlled phased array antenna applications, where long length of optical fibers are employed for true time delay devices in large apertures. In pushing these systems to the limits of transmission capability, aspects such as fiber nonlinearities need to be understood. These aspects include the nonlinear fiber phenomena of SRS (stimulated Raman scattering) [4], SBS (stimulated Brillouin scattering) [5], and XPM (cross phase modulation) [6]. These nonlinear effects become noticeable particularly in WDM subcarrier multiplexed (SCM) systems that may cover a lot of closely packed video channels cover long distances. These nonlinearities result in optical power transfer to higher and lower optical frequencies. Each nonlinear effect creates a distortion level that becomes intolerable above the acceptable threshold level. Threshold requirements are based on electrical nonlinear distortion requirements, composite second order (CSO) and composite triple beat (CTB) (particularly CTB), which have been determined in published works such as [8, 9].

Fig. 6 shows the SRS crosstalk level for a two channel WDM system, while the fiber length is varied and for 9.4 nm channel spacing, an input power of 4 dBm, a dispersion of 17 ps/nm/km, and a subcarrier frequency of 152 MHz. The two curves in the figure represent the high and low dispersion fibers. The more dispersive fiber generates lower XT due to the walk-off effect. As is expected, the crosstalk level begins to increase as the fiber length increases. However, the XT level reaches a peak value and then decreases as the length is increased further. As the length is increased beyond 70 km, eventually the SRS level reaches a steady state value. This behavior shows a sinusoidal dependence of crosstalk on fiber length for dispersive fiber but a monotonic increase in for the dispersion shifted fiber. The importance of this result is that due to the walk-off effect, the crosstalk level for a length of fiber may not increase as the fiber length increases. Hence, the crosstalk level can be reduced or increased depending upon the fiber length. In comparison of the measurement and simulation (based on Wang [8] and Phillips [9] models), the maximum error is less than 5 %. Measurement results of the

SRS crosstalk while increasing the RF frequency from 50 to 725 MHz in steps of 50 MHz is depicted in Fig. 7. Also included in the figure is a simulation of the Phillips model [9]. Figure 7 shows that as the frequency is increased, the SRS crosstalk level changes following a behavior similar to a sinc function [i.e., sinx/x] squared fashion.

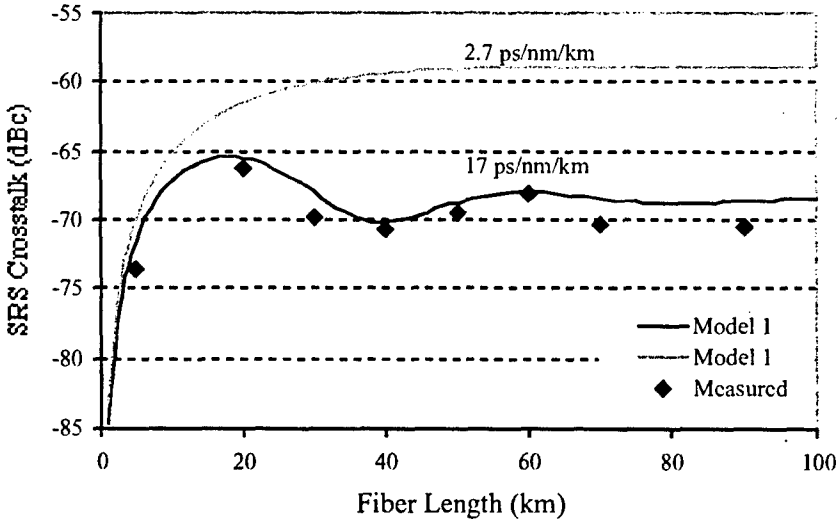

Fig. 6 Measured and simulated SRS induced crosstalk versus fiber length for an input optical power level of 4 dBm, fiber dispersion of 17 ps/nm/km, RF frequency of 151.85 MHz, and a channel spacing of 9.4 nm.

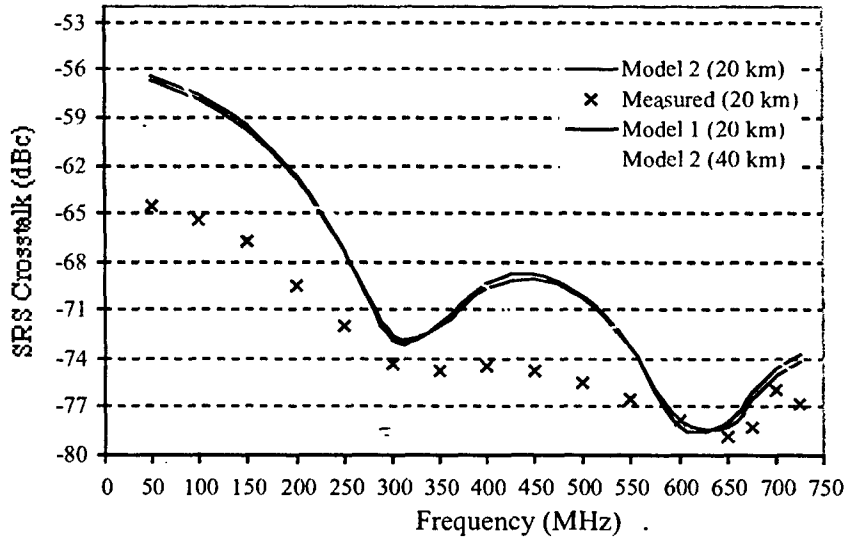

Fig. 7 Measured and simulated SRS crosstalk versus RF frequency with a fiber length of 20 km, fiber dispersion of 17 ps/nm/km, channel spacing of 9.4 nm, and a 4 dBm (2.5 mW) input power per channel, also a simulation of 40 km using only the Phillips model.

The problem of crosstalk becomes more aggravated as the number dense WDM channels increases. Even though analytical models were developed by Wang [8] to address N optical channels, but there are certain deficiencies associated with this model. An "alternative technique" was used to predict that for an 8 channel system, the crosstalk level could easily violate the acceptable cross talk. Specifically, for an input power of – 4 dBm, a subcarrier frequency of 50 MHz, a channel spacing of 1.6 nm (λ_8 = 1541.4 and $\Delta\lambda$ = 11.2 nm), and a fiber length of 40 km, the – 65 dBc threshold is violated. However,

by taking advantage of the walk-off effect, it is feasible to reduce the crosstalk level. For example, the simulation technique has predicted a greater than 10 dB decrease in crosstalk level by increasing the subcarrier frequency from 50 to 250 MHz, and decreasing the channel spacing from 1.6 to 0.8 nm. Therefore, the walk-off effect shows good potential for crosstalk reduction through control of its various parameters. The channel spacing not only affects the walk-off but also the Raman gain coefficient, thus, it offers substantial crosstalk reductions.

A four wavelength channels, ranging from 1531.90 nm to 1541.35 nm in steps of 3.2 nm, is characterized and simulated for 40 km fiber and the results are displayed in Fig. 8. The simulated curves are represented as solid lines and are labeled as XTi(2), XTi(3), XTi(4), and Alt. Tech (4), where the numbers represent the wavelength in order from the shortest wavelength (channel 1 at 1531.9 nm). In the same figure the measured and simulated crosstalk levels are presented for the second, third and fourth wavelength, while the pump wavelength is not shown (XT(1) level is expected to be much lower). Results from the measurement show some agreement with theory in that the longest wavelength channel receives the most SRS crosstalk distortion, while the shortest wavelength channel receives the smallest distortion. This alternative model provides more accuracy in the predicted distortion in a multi-channel system.

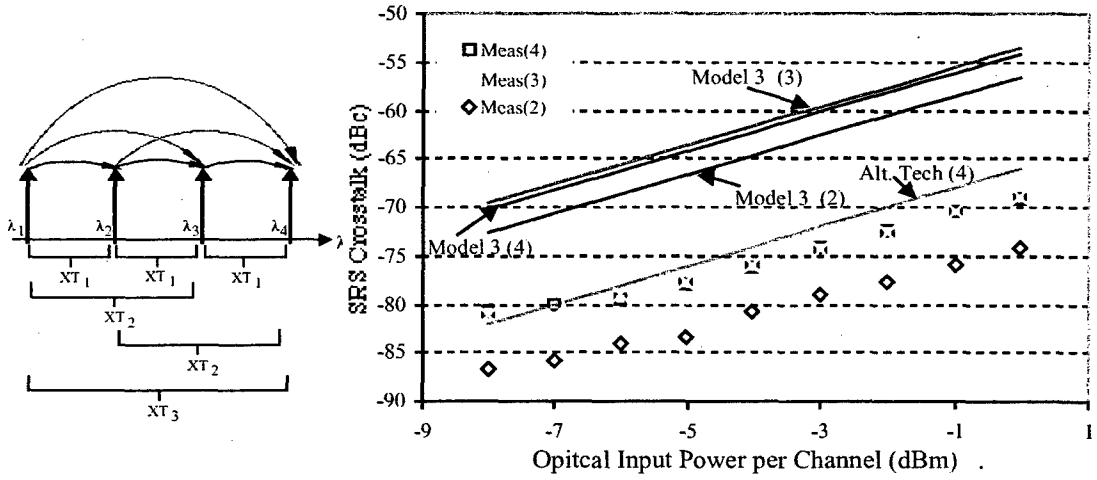

Fig. 8. Measured and simulated crosstalk versus optical input power per channel. The simulations represented include the three longest channel simulations using Wang's equation and the longest channel simulation using the alternate technique. Other parameters are a subcarrier frequency of 151.85 MHz, a dispersion of 17 ps/nm/km, a channel spacing of 9.4 nm, and a fiber length of 40 km. All discrete points are measurement points, whereas all solid lines are simulations.

Phase Noise Degradation: The FO distribution link contributes residual phase noise to the reference signal, which is a function of operation frequency. This impact is mostly significant in the directly modulated fiber optic links where the RIN of the optical source is far stronger than the externally modulated FO links. Moreover, directly modulated fiber optic links due to its lower cost than externally modulated links. The phase noise of the reference signal could be degraded if residual phase noise is too close to the signal noise floor level. Therefore, an appropriate selection of reference frequency is necessary to avoid being degraded significantly after passing through the FO link. For example as shown in Fig. 9, to generate a 12 GHz local oscillator (LO) at front-end, a reference signal at frequency of 100 MHz (UHF), 4 GHz (C-band), and 12 GHz (X-band) can be

sent through FO link. Since the phase noise contributions for FO links are different at these frequencies, an optimum frequency for reference signal can be found to have the least phase noise degradation due to FO link.

The optical spectra of a modulated optical signal are expressed as: $P_{opt}\left\{1+\mathbf{m}\cos\left(\omega_m t+\delta\phi_m(t)\right)+\mathbf{n_{RIN}}(t)\right\}\cos\left(\omega_{opt}t+\phi_{opt}(t)+\delta\phi_{opt}(t)\right)$, where P_{opt} is the averaged optical power, **m** is the optical modulation index at modulating microwave carrier, ω_m. The focus of present work is $\delta\phi_m$, the residual phase noise added to the microwave carrier from the laser diode noise source. $\mathbf{n}_{RIN}$ is the relative intensity noise; ω_{opt} is the optical frequency; ϕ_{opt} is the optical phase signal due to side modes and modulation, and $\delta\phi_{opt}$ is the phase noise of the optical signal. Since most fiber-optic links for antenna remoting applications use intensity detection, only the noise signals in optical intensity affect the microwave carrier signal, namely, $\delta\phi_m$ and $\mathbf{n}_{RIN}$. The $\mathbf{n}_{RIN}$ could contribute to the FM noise of the reference signal through nonlinear AM/PM conversion [10].

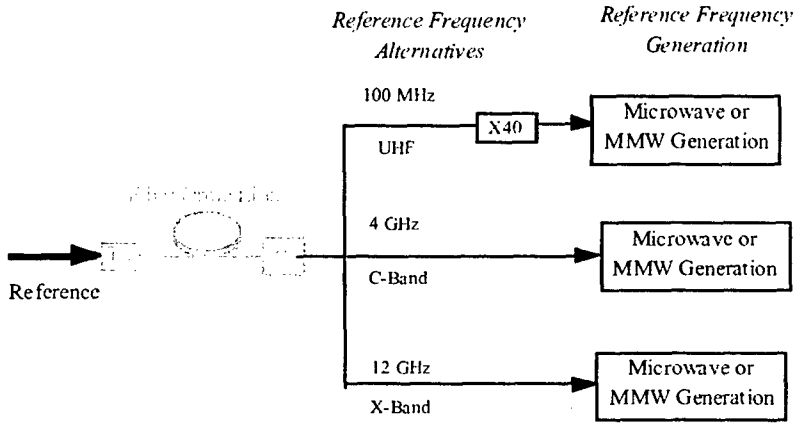

Fig. 9. Distribution of frequency reference and generation of MMW signal using various frequency references used in a FO based local oscillator (LO) synchronization network.

The laser diode SSB phase noise of the nth harmonic of the modulating signal, $\pounds_{out}$, has contributions from three noise terms: i) the input reference signal phase noise, $\pounds_{in}$; ii) the low frequency noise of laser diode up-converted to the carrier frequency, $\pounds_{up}$; and iii) the RIN noise at the offset microwave carrier, $\pounds_{RIN}$. This behavior is quite analogous to microwave systems [11]. Therefore at angular offset carrier frequency of Ω, $\pounds_{out}$ can be approximately expressed as [12]:

$$\pounds_{out,n\omega}(\Omega) = n^2\pounds_{in,\omega}(\Omega) + n^2\pounds_{up,\omega}(\Omega) + \pounds_{RIN,n\omega}(\Omega) \qquad (2)$$

The factor of n is the harmonic order of the modulation signal, if any nonlinearity of laser diode is exploited to generate the nth harmonic [10]. (If the fundamental frequency is employed then n=1.) The subscript ω indicates the modulation frequency. The up-conversion factor of low frequency RIN to phase noise is the dominant noise source. The calculation of this up-conversion factor depends on the derivative of the RF phase with respect to the RF derive amplitude and is $C_{up,\omega} = 1/2(\partial\theta(\omega)/\partial P_o)^2 P_o^2$, which θ is phase of optical signal at the modulating frequency ω. The dependence of phase on the optical output power in directly modulated system is a bit more complicated than externally modulated system since the nonlinear behavior is dependent on modulation index of laser

diode and relationship of its operation frequency compared to the relaxation oscillation frequency. This process is nonlinear and at certain frequencies results in AM-PM compression. The results are related to modulation index through "a" parameter, which is a function of modulation frequency and averaged optical power [1].

Since in semiconductor laser diodes RIN noise are strong up to 100 MHz because of mode partition noise, it is predicted that the spectral purity of the UHF reference signal is greatly degraded, resulting in a higher FM noise. Moreover, the X-band modulating signal is close to the relaxation oscillation frequency where RIN is peaked. The best frequency for reference signal distribution through DMFO link is the C-Band signal as depicted in Fig. 10, where the phase noise of the 12 GHz LO signal is generated from the reference signal through the above mentioned DMFO link. Clearly, the signal generated from a C-band signal has the best phase noise performance. The signal from UHF reference degrades greatly because the residual phase noise of the FO link is higher than the reference phase noise at offset frequency higher than 100 Hz.

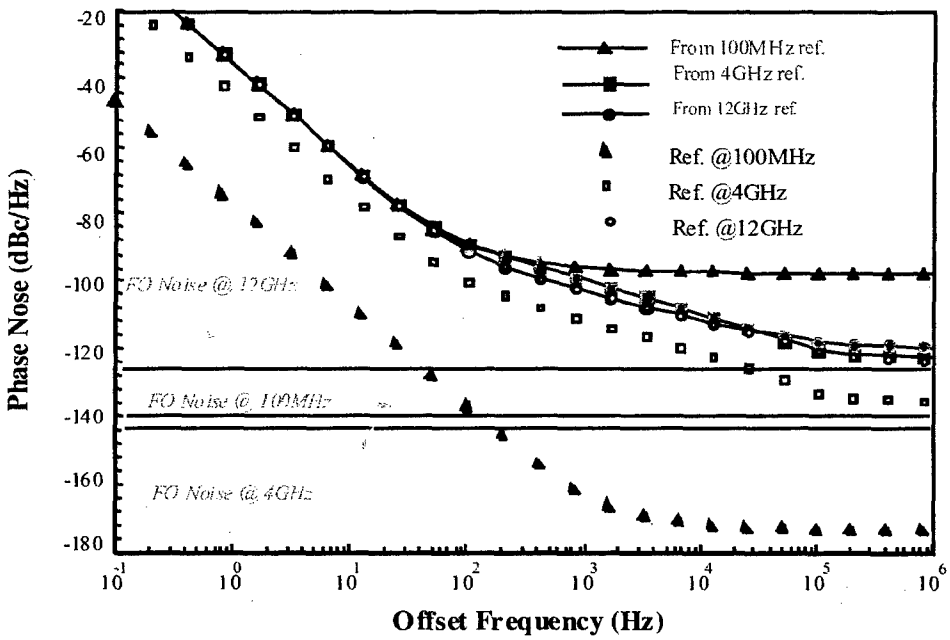

Fig. 10. The simulated phase noise of a LO signal at 12 GHz, which is generated from different reference signals through a directly modulated FO link as depicted in Fig. 9.

3.0. Semiconductor Laser Diodes with Self-Resonance

It is attractive to achieve optical systems that provide a performance analogous to the electrical functions. For example, a laser source with oscillation at millimeter wave frequencies along with the opto-electronic mixing would resemble the SOM circuit. A F-P laser with optical feedback has provided this feature and was first reported by Lau [13]. This resonance frequency is stabilized using a modulating frequency fundamentally or harmonically related to the self-resonance frequency. A thorough characterization and explanation of FM noise degradation of the frequency reference in the laser is also reported by Ni et al [12].

A monolithic version of laser with external cavity is realizable using semiconductor fabrication process and reported by a number of researchers. Fig. 11a shows a schematic drawing of the monolithic laser with an integrated EA modulator. Stacked structure consisting of two MQW layers, a MQW for laser diode (MQW-LD) and a MQW for EA

modulator (MQW-MD) are employed. The F-P cavity length for our experiment is cleaved approximately for a length of 2170μm. This total length is composed of 1970 μm long gain section, 150 μm long modulator, and a 50 μm long separation region. The facet of the modulator section is coated with high reflective film (R≈85%). The facet of the gain section is as cleaved. The laser is mounted in a high-frequency package. The schematic diagram of the long FP laser with integrated EA modulator is shown in Fig. 11b.

The gain section of the laser diode is forward biased at different bias currents and the EA section is reverse-biased by different voltage levels. The natural frequency response of the laser is measured at various laser bias currents, ranging from I_b=80mA up to I_b=150mA for bias voltage of V_m=0V. A resonance peak is observed that is associated with the longitudinal mode separation in the long FP laser. The longitudinal mode separation is calculated as $\Delta f = c/2nL \approx 19.3$GHz, where c=300mm.GHz is speed of light in free space, n≈3.5 is index of refraction of wave-guide, and L≈2.17mm is the F-P cavity length. This resonant frequency has a frequency tuning sensitivity of ≈1MHz/mA.

One could stabilize the optical oscillations using injection-locking process as demonstrated [13]. As the gain section is modulated by a synthesized frequency reference (HP83640A) of P_m≈-1dBm at f_m=19.258GHz, a single oscillation peak appears. The familiar one-sided injection-locking spectra are observed outside the injection locking range and the close-in to carrier phase noise is significantly reduced within the locking range. The measured close in to carrier phase noise degradation at 100Hz offset carrier is depicted in Fig. 12, where 31dB and 6dB degradation are measured for the injected power of P_m=+0.5dBm in the resistively- and reactively-matched modules respectively. However for injected power level of +4.5dBm, a close-in to carrier phase noise identical to the reference source is measured for the reactively-matched case.

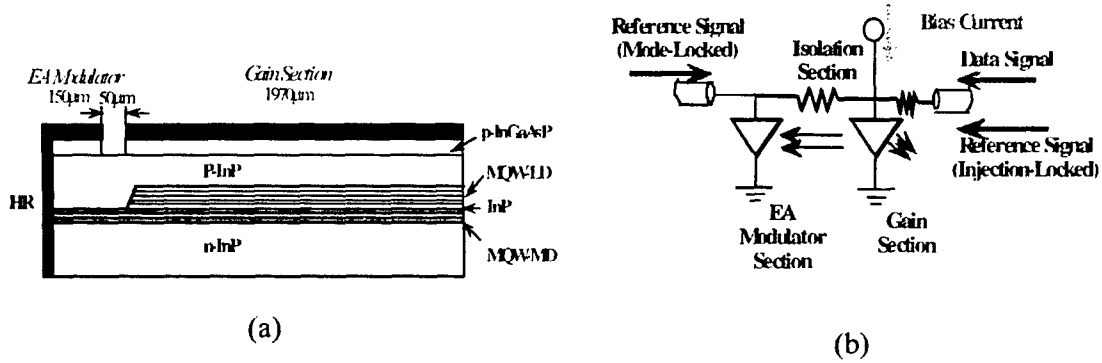

Fig. 11. a) Conceptual representation of the long F-P laser integrated with an electro-absorption modulator; b) mechanical fixture used for mounting of the laser diode for injection locking, mode locking and opto-electronic conversion evaluations.

The 19.3 GHz resonant frequency has a frequency tuning sensitivity of ≈1MHz/mA. The resonance frequency is stabilized using fundamental mode-locking by modulating the EA section by a synthesized source. The close-in to carrier phase noise are measured and comparison is made against the reference signal from an HP83640A source. The results are summarized in Table I for different laser operation points. As indicated a very small phase noise degradation is observed, however the results for V_m= – 1 V is better that the results for V_m =-4.5V for the same laser current of I_b=140mA.

		£(Ω)(dBc/Hz)		Δ(dB)	
f_m (GHz)	V_m (V)	Ω=100Hz	Ω=1kHz	Ω=100Hz	Ω=1kHz
19.13400	-4.5	-75.4	-81	2.6	2.4
19.29469	-2.5	-77.0	-82	1.0	1.1
19.29406	-1.0	-77.6	-82	0.4	0.4

Table I. Phase noise degradation of the LO signal as a function of various offset frequencies and laser operation points.

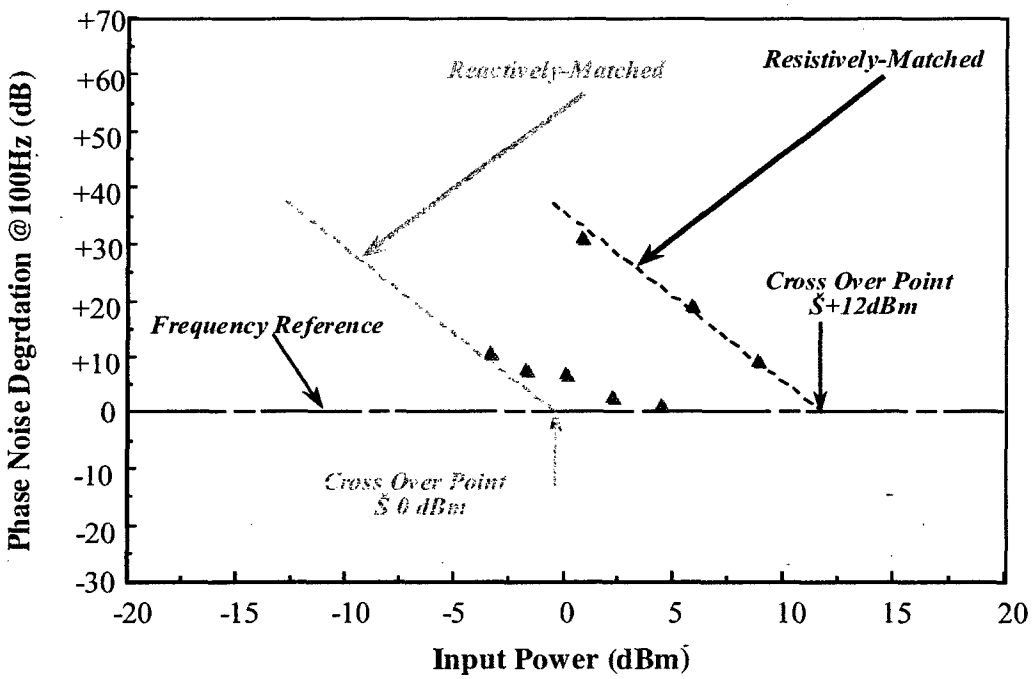

Fig. 12. Measured FM noise degradation at 100Hz offset carrier for the injection locked intermodal oscillation. The measured injection locking power of the long F-P laser diode are also depicted at the cross over point for the resistively- (▲) and reactively-matched (▲) lasers.

Since this stabilized signal has much cleaner close-in to carrier phase noise than the free-running oscillation, it could be employed as the LO signal. The laser diode's gain section is forward biased (I_b = 140 mA) and the EA modulator section is reverse biased (V_m = -1V). This operating point is selected because of the efficient mode-locking process while maintaining the least amount of phase noise degradation of the carrier signal. The laser diode optical output is collimated to a single mode optical fiber using a polarizing collimator with an overall fiber coupling efficiency of 12%. The optical fiber output is connected to an optical receiver integrated with RF analyzer (HP70004A system). Note that HP70004A system automatically de-embeds the calibrated optical

receiver response from the measurement and displays it in the optical domain. The electrical domain power levels, in dBr, are easily calculated by multiplying the depicted optical domain results, displayed in dBm, by a factor of 2.

Next the gain section of this laser is modulated by S-band signals (2.2 GHz ± 50 MHz). Strong nonlinearity of the mode-locked laser at the LO signal of 19.3 GHz up-converts the S-band signals to 17.1 GHz and 22.5 GHz as shown in Fig. 13. The data modulation power level is changed over a wide range. An optical conversion loss is defined as the ratio of the generated mixed RF signal (19.3 ± 2.2 GHz) to the IF signal (2.2 GHz). The optical conversion loss is as low as 1.4 dB resulting in the electrical conversion loss of 2.8 dB. The opto-electronic conversion loss for the lower side-band (LSB) at 17.1 GHz is higher than the upper side-band (USB) of 22.5 GHz by 1.3 dB (i.e., 2.6 dB electrical) [14].

On the other hand, a modulation loss greater than 51 dB is measured when the gain section is directly modulated by the RF signal at 17.1 GHz. The spurious-free dynamic range (SFDR) of this opto-electronic mixer is also evaluated. The intermodulation distortion (IMD) measurements are conducted for two modulating tones which are 5 MHz apart (e.g., f_1 = 2.200 GHz and f_2 = 2.205 GHz). Both tones are up-converted by stable LO signal of 19.360 GHz and IMD of the up-converted RF signals are measured at LSB and USB frequencies. Based on the mode-locked laser IMD and RIN noise measurement results for the up-converted RF tones, SFDR LSB and USB RF signals are ≈ 88 dB.$Hz^{2/3}$ and 89 dB.$Hz^{2/3}$ respectively.

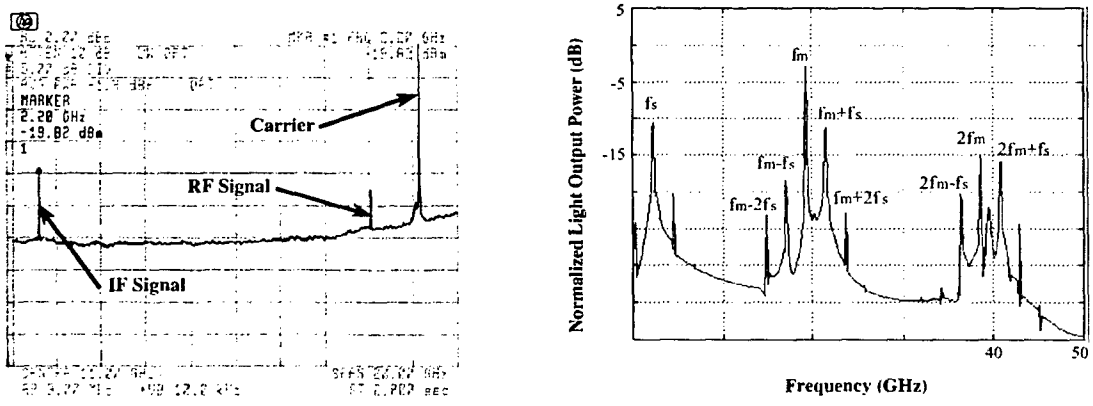

(a) (b)

Fig. 13. Opto-electronic mixing of data signal with local oscillator signal in the mode-locked long FP laser diode. a) Experimental results for the operating condition is I_b = 140 mA, V_m = -1 V, f_m = 19.360 GHz, P_m = +15 dBm, f_{data} = 2.200 GHz, and P_{data} = -25 dBm. Data, lower side-band RF, and local oscillator signals (center frequency of 11.0 GHz and frequency span of 20.0 GHz); b) simualtion results based on travelling wave rate equation [15].

4.0. CONCLUSIONS

Fiber fed wireless communication is considered for mobile and fixed-point communications in micro and pico-cellular as well as many military ad-hoc WLAN scenarios. This paper has addressed fiber optic distribution of analog data in terms of link gain and dynamic range and frequency reference signal for generation of a coherent local oscillator signal in terms of AM/PM conversion. Moreover, distortion induced by SRS in

dense WDM systems is discussed. Fiber optic links based on directly modulated could meet cost-performance for many applications, even though monolithically integrated EA modulators are becoming very attractive. (This topic is discussed in a paper in this proceedings dealing with the state-of the-art of devices and circuits by Prof. Dieter Jaeger.)

A monolithically integrated FP laser with EA modulator is employed to simultaneously transmit frequency reference of data signals. The analytical models indicate that stabilized LO signal at 19.3 GHz can be attained using injection locking and mode-locking. The achieved close-in to carrier phase noise of the stabilized LO signal is lower in the case of injection locking than mode-locking for the same modulating power level. The opto-electronic mixing of 19.2 GHz LO and S-band data is also feasible using this device with SFDR as high as 90 dB. $Hz^{2/3}$. Moreover, optoelectrnic mixing can occur in a mode-locked laser, creating possibility of generating RF signal from frequency reference and data signals, thus bypassing the need for integration with electrical mixers in the up- and down-conversion. (A similar approach using attractive microchip laser is presented in this proceedings by Prof. Tibor Berceli.)

ACKNOWLEDGMENT

The author wishes to acknowledge the contribution of many of his students, partciularly Dr. Edward Ackerman, Mr. Adam McInvale, Dr. Tsang Der Ni, Dr. Xiangdong Zhang, and Dr. Joong Hee Lee.

REFERENCES

[1] A. S. Daryoush, E. Ackerman, N. Samant, D. Kasemsat, S. Wanuga, "Interfaces for High-Speed Fiber Optic Links: Analysis and experiment," *IEEE Trans. on Microwave Theory and Techniques,* vol. 39, no. 12, Dec. 1991.

[2] Edward Ackerman, Photonics Inc., Private Communications.

[3] K. Emura, "Technological Choices in Optical Fiber Feeding Wireless Access Systems," Microwave Photonics Satellite Workshop, Dec. 1996, Kyoto, Japan.

[4] A.R. Chraplyvy, P. S. Henry, "Performance degradation due to stimulated Raman scattering in wavelength-division-multiplexed optical-fiber systems," *Electron Lett.*, Vol. 19, No 16, August 1983.

[5] A.R. Chraplyvy, "Limitations on Lightwave Communications Imposed by Optical-Fiber Nonlinearities," *J. of Lightwave Technology*, Vol. 8, No. 10, Oct. 1990.

[6] Z. Wang, et. al., "Effects of Cross Phase Modulation in Wavelength SCM Video Transmission Systems," *Electronics Lett.*, Vol. 31, No. 18, August 1995.

[7] T. E. Darcie et. al., "Lightwave Multi-channel Analog AM Video Distribution Systems,"*IEEE International Conference on Communications*, Boston, MA, June 1989.

[8] Z. Wang, A. Li, C.J. Mahon, G. Jacobsen, and E. Bodtker "Performance Limitations imposed by Stimulated Raman Scattering in Optical WDM SCM Video Distribution Systems", *IEEE Photonics Techn. Lett.*, Vol. 7, No. 12, December 1995.

[9] M.R. Phillips and D.M. Ott, "Crosstalk Due to Optical Fiber Nonlinearities in WDM CATV Lightwave Systems," *J. of Lightwave Technology*, Vol. 17, No. 10, Oct. 1999.

[10] X. Zhang, T.D. Ni, and A.S. Daryoush, "Laser Induced Phase Noise in Optically Injection Locked Oscillator," *Digest of IEEE 1992 MTT Symposium*, pp.765-768, 1992.

[11] X. Zhang and A.S. Daryoush, "Bias Dependent Low Frequency Noise Up-Conversion in HBT Oscillators", *IEEE Microwave and Guided wave Letters,* vol. 4, no. 12, pp. 423-425, Dec. 1994.

[12] T.D. Ni, X. Zhang, and A.S. Daryoush, "Experimental Study on Close-in carrier Phase Noise of Laser Diode with Coherent Feedback," *IEEE Trans. Microwave Theory and Techniques*, vol. 43, no. 9, pp. 2277-2283, Sept. 1995.

[13] K. Lau, "Short-Pulse and High-frequency Signal Generation in Semiconductor Lasers," *IEEE Journal of Lightwave Technology*, Vol. 7, No. 2, pp. 400-419, Feb. 1989.
[14] A.S. Daryoush, K. Sato, K. Horikawa, and H. Ogawa, "Efficient Opto-electronic Mixing at Ka-Band using a Mode-locked Laser," *IEEE Microwave and Guided Wave Lett.*, vol. 9, no. 8, pp. 317-319, August 1999.
[15] A. S. Daryoush, et al., "Applications of Opto-Electronic Mixing in Distributed Systems" Digest of *2001 Topical Symposium on Millimeter Wave, TSMMW2001*, Yokosuka, Japan, pp. 175 – 178, March 2001.